J|A|C|S
ARTICLES
Published on Web 09/14/2004

Accelerated Color Change of Gold Nanoparticles Assembled by DNAzymes for Simple and Fast Colorimetric Pb^{2+} Detection

Juewen Liu and Yi Lu*

Contribution from the Department of Chemistry, University of Illinois at Urbana-Champaign, Urbana, Illinois 61801

Received June 8, 2004; E-mail: yi-lu@uiuc.edu

Abstract: The combination of high metal selectivity of DNAzymes with the strong distance-dependent optical properties of metallic nanoparticles has presented considerable opportunities for designing colorimetric sensors for metal ions. We previously communicated a design for a colorimetric lead sensor based on the assembly of gold nanoparticles by a Pb^{2+}-dependent DNAzyme. However, heating to 50 °C followed by a cooling process of ~2 h was required to observe the color change. Herein we report a new improved design that allows fast (<10 min) detection of Pb^{2+} at ambient temperature. This improvement of sensor performance is a result of detailed studies of the DNAzyme and nanoparticles, which identified "tail-to-tail" nanoparticle alignment, and large (42 nm diameter) nanoparticle size as the major determining factors in allowing fast color changes. The optimal conditions for other factors such as temperature (35 °C) and concentrations of the DNAzyme (2 μM), its substrate (3 nM), and NaCl (300 mM) have also been determined. These results demonstrate that fundamental understanding of the DNAzyme biochemistry and nanoparticle science can lead to dramatically improved colorimetric sensors.

Introduction

Metal ion sensor design has been a focus of many research endeavors, as it can provide detection and quantification of metal ions in many fields of application such as environmental bioinorganic chemistry, developmental biology, clinical toxicology, waste management, and bioremediation of radionuclides and metal ions.[1−12] While significant progress has been made on the design of sensors using fluorescence,[1−3,5−7,9−13] surface plasmon resonance,[4] electrochemistry,[8] and other detection techniques,[14,15] designing colorimetric sensors is much less advanced, even though colorimetric sensors can allow onsite, real-time qualitative or semiquantitative detection without complicated analytical instruments.[16−19]

With recent developments in nanotechnology and biology, new methods of designing colorimetric biosensors are emerging.[16,20,21] In nanotechnology, the assembly of metallic nanoparticles has resulted in novel materials with interesting properties.[22−24] The extremely high extinction coefficients and the strongly distance-dependent optical properties of gold nanoparticles allow the nanoparticles to be utilized as ideal color reporting groups for colorimetric sensor design.[16,25] For example, the extinction coefficients of 13- and 50-nm diameter gold nanoparticles are 2.7×10^8 and 1.5×10^{10} M^{-1} cm^{-1} (at ~520 nm), respectively,[26] which are 3−5 orders of magnitude more than those of traditional organic chromophores. As a result, nanoparticles at nanomolar concentration can be clearly observed by naked eyes, allowing sensitive detection with minimal consumption of materials. More importantly, when gold nanoparticles approach each other and aggregate, the color of the nanoparticles changes from red to blue, because of the shift of the surface plasmon band to longer wavelength. When gold

(1) Walkup, G. K.; Imperiali, B. *J. Am. Chem. Soc.* **1996**, *118*, 3053−3054.
(2) Miyawaki, A.; Llopis, J.; Helm, R.; McCaffery, J. M.; Adams, J. A.; Ikura, M.; Tsien, R. Y. *Nature* **1997**, *388*, 882−887.
(3) Henary, M. M.; Fahrni, C. J. *J. Phys. Chem. A* **2002**, *106*, 5210−5220.
(4) Homola, J.; Yee, S. S.; Gauglitz, G. *Sens. Actuators B* **1999**, *B54*, 3−15.
(5) Deo, S.; Godwin, H. A. *J. Am. Chem. Soc.* **2000**, *122*, 174−175.
(6) Li, J.; Lu, Y. *J. Am. Chem. Soc.* **2000**, *122*, 10466−10467.
(7) Chen, P.; He, C. *J. Am. Chem. Soc.* **2004**, *126*, 728−729.
(8) Turner, A. P. F. *Science* **2000**, *290*, 1315−1317.
(9) Burdette, S. C.; Walkup, G. K.; Spingler, B.; Tsien, R. Y.; Lippard, S. J. *J. Am. Chem. Soc.* **2001**, *123*, 7831−7841.
(10) Woodroofe, C. C.; Lippard, S. J. *J. Am. Chem. Soc.* **2003**, *125*, 11458−11459.
(11) Nolan, E. M.; Lippard, S. J. *J. Am. Chem. Soc.* **2003**, *125*, 14270−14271.
(12) Liu, Z.; Mei, S. H. J.; Brennan, J. D.; Li, Y. *J. Am. Chem. Soc.* **2003**, *125*, 7539−7545.
(13) Zhao, X.; Tapec-Dytioco, R.; Tan, W. *J. Am. Chem. Soc.* **2003**, *125*, 11474−11475.
(14) *Optical Biosensors: Present and Future*; Ligler, F. S., Taitt, C. A., Eds.; Elsevier Science: Amsterdam, 2002.
(15) Blake, D.; Chakrabarti, P.; Khosraviani, M.; Hatcher, F. M.; Westhoff, C. M.; Goebel, P.; Wylie, D. E.; Blake, R. C., II. *J. Biol. Chem.* **1996**, *271*, 27677−27685.
(16) Elghanian, R.; Storhoff, J. J.; Mucic, R. C.; Letsinger, R. L.; Mirkin, C. A. *Science* **1997**, *277*, 1078−1080.
(17) Stojanovic, M. N.; Landry, D. W. *J. Am. Chem. Soc.* **2002**, *124*, 9678−9679.
(18) Nam, J.-M.; Thaxton, C. S.; Mirkin, C. A. *Science* **2003**, *301*, 1884−1886.
(19) Ho, H.-A.; Leclerc, M. *J. Am. Chem. Soc.* **2004**, *126*, 1384−1387.
(20) Liu, J.; Lu, Y. *J. Am. Chem. Soc.* **2003**, *125*, 6642−6643.
(21) Liu, J.; Lu, Y. *Anal. Chem.* **2004**, *76*, 1627−1632.
(22) Mirkin, C. A.; Letsinger, R. L.; Mucic, R. C.; Storhoff, J. J. *Nature* **1996**, *382*, 607−609.
(23) Alivisatos, A. P.; Johnsson, K. P.; Peng, X.; Wilson, T. E.; Loweth, C. J.; Bruchez, M. P., Jr.; Schultz, P. G. *Nature* **1996**, *382*, 609−611.
(24) Chen, S. *Adv. Mater.* **2000**, *12*, 186−189.
(25) Storhoff, J. J.; Lazarides, A. A.; Mucic, R. C.; Mirkin, C. A.; Letsinger, R. L.; Schatz, G. C. *J. Am. Chem. Soc.* **2000**, *122*, 4640−4650.
(26) Jin, R.; Wu, G.; Li, Z.; Mirkin, C. A.; Schatz, G. C. *J. Am. Chem. Soc.* **2003**, *125*, 1643−1654.

10.1021/ja046628h CCC: $27.50

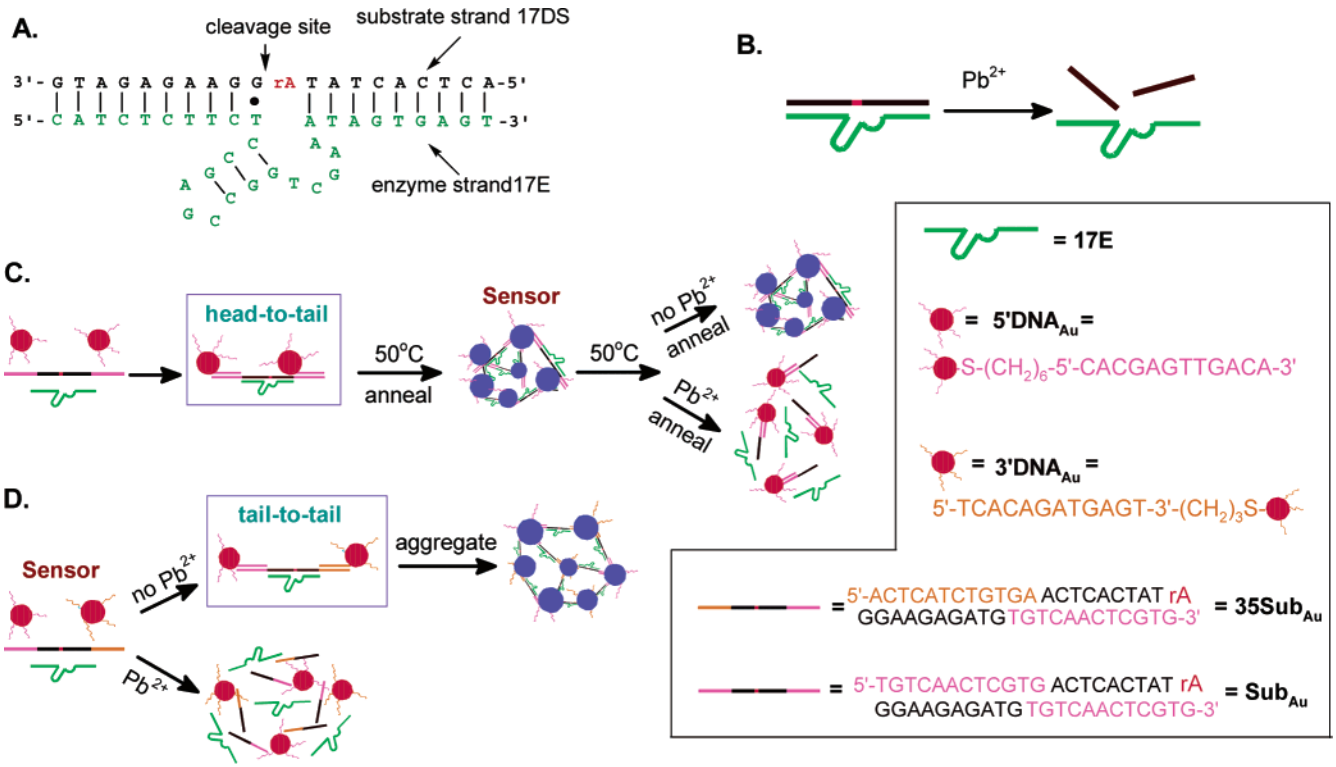

Figure 1. (A) Secondary structure of the "8−17" DNAzyme. (B) Cleavage of 17DS by 17E in the presence of Pb^{2+}. (C) Schematics of the previous colorimetric Pb^{2+} sensor design. The three components of the sensor (5′DNA_{Au}, Sub_{Au}, and 17E) can assemble to form blue-colored aggregates. Nanoparticles were aligned in a "head-to-tail" manner. A heating-and-cooling process (annealing) was needed for detection. (D) Schematics of the new colorimetric sensor design. The nanoparticles are aligned in the "tail-to-tail" manner. In the absence of Pb^{2+}, nanoparticles can be assembled by the DNAzyme at ambient temperature within 10 min, resulting in a blue color; while in the presence of Pb^{2+}, $35Sub_{Au}$ is cleaved by 17E, inhibiting the assembly, resulting in a red color of separated nanoparticles.

nanoparticles are functionalized with thiol-modified DNA, the distance between gold nanoparticles can be controlled by a linking DNA that is complementary to the DNA attached to nanoparticles.[22] On the basis of this phenomenon, colorimetric biosensors for highly sensitive and selective detection of complementary DNA have been developed.[16,27]

In biology, DNA has been shown to no longer be just a purely genetic material; it can catalyze a number of reactions in the manner seen for protein- or RNA-based biocatalysts. Catalytically active DNA molecules are known as deoxyribozymes or DNAzymes.[28−32] DNAzymes are attractive molecules for metal ion sensor design because DNAzymes with metal-dependent activities can be conveniently obtained through combinatorial biology methods such as systematic evolution of ligands by exponential enrichment (SELEX) or in vitro selection.[33−38] For example, DNAzymes that are specific for Pb^{2+},[28] Cu^{2+},[39−41] Zn^{2+},[42] and Co^{2+} [43,44] have already been obtained. For practical applications, DNA molecules are much more stable than protein or RNA and can be denatured and renatured many times without losing activity or binding ability. DNA is also cost-effective to produce. With these valuable properties, DNAzymes have already shown promising applications as anti-viral agents,[45] components for DNA-based logic gates,[46] as well as components for biosensors.[6,32,43,47]

By using a Pb^{2+}-specific DNAzyme as the target recognition element and DNA-functionalized gold nanoparticles as the signaling element, we communicated a design of a colorimetric Pb^{2+} biosensor.[20] The Pb^{2+}-specific DNAzyme is known as the "8−17" DNAzyme,[45,48,49] whose secondary structure is shown in Figure 1A. The DNAzyme is composed of a substrate strand (17DS) and an enzyme strand (17E). Both strands are DNA, except that the substrate strand contains a single RNA linkage (ribonucleoside adenosine, (rA)) that serves as the cleavage site. In the presence of Pb^{2+}, the substrate strand is cleaved by the enzyme strand (Figure 1B). At pH 6.0, the single-turnover rate

(27) Chakrabarti, R.; Klibanov, A. M. *J. Am. Chem. Soc.* **2003**, *125*, 12531−12540.
(28) Breaker, R. R.; Joyce, G. F. *Chem. Biol.* **1994**, *1*, 223−229.
(29) Breaker, R. R. *Nat. Biotechnol.* **1997**, *15*, 427−431.
(30) Sen, D.; Geyer, C. R. *Curr. Opin. Chem. Biol.* **1998**, *2*, 680−687.
(31) Breaker, R. R. *Science* **2000**, *290*, 2095−2096.
(32) Lu, Y. *Chem.−Eur. J.* **2002**, *8*, 4588−4596.
(33) Ellington, A. D.; Szostak, J. W. *Nature* **1990**, *346*, 818−822.
(34) Gold, L.; Polisky, B.; Uhlenbeck, O.; Yarus, M. *Annu. Rev. Biochem.* **1995**, *64*, 763−797.
(35) Osborne, S. E.; Ellington, A. D. *Chem. Rev.* **1997**, *97*, 349−370.
(36) Breaker, R. R. *Chem. Rev.* **1997**, *97*, 371−390.
(37) Wilson, D. S.; Szostak, J. W. *Annu. Rev. Biochem.* **1999**, *68*, 611−647.
(38) Joyce, G. F. In *The RNA World*, 2nd ed.; Gesteland, R. F., Cech, T. R., Atkins, J. F., Eds.; Cold Spring Harbor Laboratory Press: Cold Spring Harbor, New York, 1999; Vol. 37, pp 687−689.
(39) Cuenoud, B.; Szostak, J. W. *Nature* **1995**, *375*, 611−614.
(40) Carmi, N.; Shultz, L. A.; Breaker, R. R. *Chem. Biol.* **1996**, *3*, 1039−1046.
(41) Wang, W.; Billen, L. P.; Li, Y. *Chem. Biol.* **2002**, *9*, 507−517.
(42) Santoro, S. W.; Joyce, G. F.; Sakthivel, K.; Gramatikova, S.; Barbas, C. F., III. *J. Am. Chem. Soc.* **2000**, *122*, 2433−2439.
(43) Mei, S. H. J.; Liu, Z.; Brennan, J. D.; Li, Y. *J. Am. Chem. Soc.* **2003**, *125*, 412−420.
(44) Bruesehoff, P. J.; Li, J.; Augustine, I. A. J.; Lu, Y. *Combinat. Chem. High Throughput Screening* **2002**, *5*, 327−335.
(45) Santoro, S. W.; Joyce, G. F. *Proc. Natl. Acad. Sci. U.S.A.* **1997**, *94*, 4262−4266.
(46) Stojanovic, M. N.; Mitchell, T. E.; Stefanovic, D. *J. Am. Chem. Soc.* **2002**, *124*, 3555−3561.
(47) Fahlman, R. P.; Sen, D. *J. Am. Chem. Soc.* **2002**, *124*, 4610−4616.
(48) Faulhammer, D.; Famulok, M. *Angew. Chem., Int. Ed. Engl.* **1996**, *35*, 2837−2841.
(49) Li, J.; Zheng, W.; Kwon, A. H.; Lu, Y. *Nucleic Acids Res.* **2000**, *28*, 481−488.

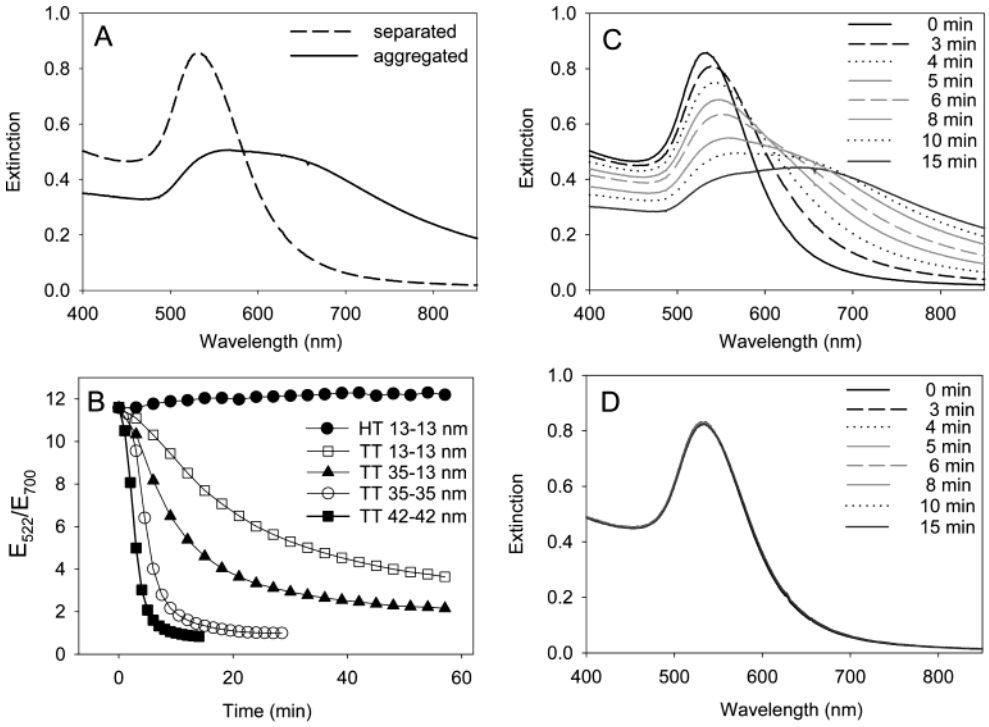

Figure 2. (A) Extinction spectra of separated (dashed curve) and DNAzyme assembled (solid curve) 42-nm gold nanoparticles. The experimental conditions were 3 nM $35Sub_{Au}$, 2 μM 17E, 300 mM NaCl, pH 8.2, and 35 °C. (B) The effect of nanoparticle alignment and size on the rate of color change. Extinction ratios were normalized for comparison. In the figure legends, "HT" and "TT" denote "head-to-tail" and "tail-to-tail" alignment, respectively. The two numbers following indicate the sizes of nanoparticles used. The experiments were performed with 2 μM 17E at room temperature. The substrate concentration was 160 nM for 13-nm nanoparticles, 120 nM for 13−35-nm mixed nanoparticles, and 3 nM for 35−35 nm and 42−42 nm nanoparticles. Time-dependent extinction spectra for the DNAzyme-assembled gold nanoparticles (C) in the absence of Pb^{2+} or (D) in the presence of 4 μM of Pb^{2+}. Experimental conditions were the same as described in Figure 2A.

constant for the cleavage reaction was determined to be ~7 min^{-1} with saturated Pb^{2+}. A linear pH-dependent behavior of the DNAzyme suggested that at higher pH, the cleavage reaction would be even faster (~220 min^{-1} at pH 7.5).[50] To adapt the DNAzyme into a colorimetric Pb^{2+} sensor, the substrate strand was extended on both ends by 12 bases, which were complementary to a 12-mer DNA attached to gold nanoparticles. The nanoparticles ($5'DNA_{Au}$), extended substrate (Sub_{Au}), and enzyme (17E) could assemble to form blue-colored aggregates and be used as a colorimetric sensor for Pb^{2+}. To sense Pb^{2+}, the aggregates were warmed to a temperature above their melting temperature (T_m = 46 °C for the aggregates in 300 mM NaCl), at which the aggregates were dissociated into separated nanoparticles, resulting in a red color. If the system was allowed to cool slowly to room temperature in the absence of Pb^{2+}, the nanoparticles could re-assemble to form blue aggregates. If Pb^{2+} was present, the substrate was cleaved by the enzyme in the cooling process, inhibiting the reformation of nanoparticle aggregates and resulting in a red color (Figure 1C). Therefore, by observing the color of the sensor, Pb^{2+} could be detected and quantified.[20]

This colorimetric sensor was highly sensitive and selective for Pb^{2+} and showed an interesting tunable detection range.[20,51] However, there are several disadvantages for this design. For example, heating was required, followed by a cooling process of ~2 h to observe color changes, which made practical onsite applications difficult. Here we report a new improved design that allows fast (<10 min) detection of Pb^{2+} at ambient temperature. By dramatically improving the performance of the colorimetric sensor, we demonstrate the impact of a detailed understanding of both DNAzyme biology and nanoparticle technology on sensor design.

Results and Discussion

Ratiometric Quantification of Colorimetric Signals. The signaling of the colorimetric sensor is based on the color change of gold nanoparticles at different assembly states. Therefore, it is very important to find a simple, yet reliable method to quantify the optical properties of gold nanoparticles. Dispersed 13-nm gold nanoparticles possess a surface plasmon peak at 522 nm. For larger particles, the peak shifts to longer wavelength (e.g., 532 nm for 42-nm nanoparticles). In Figure 2A, extinction spectra of separated (dashed curve) and aggregated (solid curve) 42-nm gold nanoparticles are presented. Upon aggregation, the 532-nm peak decreases in intensity while the extinction in the 700-nm region increases (solid curve), resulting in the red-to-blue color transition.[25] On the basis of previous experiments,[20,21,51] it was found that quantitative results could be obtained by monitoring the ratio of extinction at the plasmon peak (532 nm) and at 700 nm. A higher ratio was associated with separated nanoparticles of red color, while a lower ratio was associated with aggregated nanoparticles of blue color. Although the extinction ratio differed slightly for nanoparticles prepared in different batches, the trend of the extinction ratio change with respect to the assembly state of nanoparticles was maintained. Therefore, instead of using the change of extinction at a single wavelength, the ratiometric method was used to

(50) Brown, A. K.; Li, J.; Pavot, C. M. B.; Lu, Y. *Biochemistry* **2003**, *42*, 7152−7161.
(51) Liu, J.; Lu, Y. *Chem. Mater.* **2004**, *16*, 3231−3238.

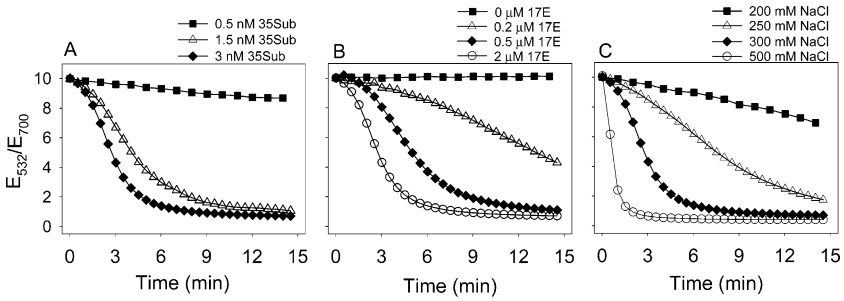

Figure 3. Optimization of the Pb^{2+} sensor system. (A) Effect of the substrate concentration on the rate of aggregation (at 35 °C). NaCl and 17E concentration were 300 mM and 2 μM, respectively. (B) Effect of the enzyme (17E) concentration on the rate of aggregation. The substrate concentration was 3 nM, and other conditions are the same as those in (A). (C) Effect of NaCl concentration on the rate of aggregation. The substrate concentration was 3 nM, and other conditions are the same as those in (A).

monitor the assembly state of gold nanoparticles. Ratiometric sensors such as this are suitable for practical applications since they are less vulnerable to fluctuations of sampling and monitoring conditions.

New Sensor Design with Accelerated Rate of Color Change. In the previous sensor design (Figure 1C),[20] a heating-and-cooling process was required because the three components of the sensor (5′DNA_{Au}, Sub_{Au}, and 17E) did not assemble spontaneously at room temperature. For example, by monitoring the extinction ratio of the above system for an hour at room temperature, no change could be observed (Figure 2B, ●) The assembly could only be observed when a heating-and-cooling process was employed, as it facilitated DNA hybridization.[20,51] To improve the performance of the sensor, we investigated the effect of nanoparticle alignment on the rate of nanoparticle aggregation. In the original design, the nanoparticles were aligned in a "head-to-tail" manner (Figure 1C). This alignment made it easy to synthesize the DNA-functionalized nanoparticles because both the "head" and "tail" had the identical DNA sequence, and therefore only one set of the DNA-functionalized nanoparticles was needed to hybridize to the DNAzyme substrate (Sub_{Au}). However, we argue that this design, albeit simple, might result in a large steric hindrance that could disfavor the assembly. Indeed, by changing DNA sequences to allow nanoparticles to be aligned in the "tail-to-tail" manner (Figure 1D), nanoparticle aggregation could be observed at room temperature (Figure 2B, □). However, the rate of aggregation was still slow, and more than 1 h was needed for the aggregation to reach completion.

To accelerate the rate of color change, nanoparticles with larger sizes were then employed. It is known that the optical properties of a nanoparticle aggregate are dominated by its size, instead of the number of nanoparticles in the aggregate.[25,52] Therefore, less aggregation should be required to give the same color change with larger nanoparticles, and the time required for the color change should be decreased. This was indeed what was observed. For example, the rates of color change were progressively faster for a mixture of 13- and 35-nm nanoparticles (Figure 2B, ▲), all 35-nm nanoparticles (○), and all 42-nm nanoparticles (■). The color change approached completion in less than 10 min for 42-nm nanoparticles. Therefore, by using a "tail-to-tail" alignment and larger nanoparticles, a room-temperature aggregation-based sensor was designed (Figure 1D). The new sensor system was composed of the enzyme (17E), an extended substrate ($35Sub_{Au}$), and two kinds of nanoparticles (5′DNA_{Au} and 3′DNA_{Au}), which were functionalized with 5′- and 3′-end thiol-modified 12-mer DNA, respectively. The nanoparticles were arranged in a "tail-to-tail" manner. In the absence of Pb^{2+}, the nanoparticles assembled gradually, accompanied by a color change from red to blue. Figure 2C shows the extinction spectra of the sensor system at different time points in the absence of Pb^{2+}. A decrease of the 532-nm peak and the increase of extinction at 700 nm could be observed. If Pb^{2+} was present, the substrate was cleaved by the enzyme, inhibiting nanoparticle aggregation (Figure 2D).

Optimization of the New Pb^{2+} Sensor System. Since the rate of color change is crucial for practical applications of the sensor, factors that affect the rate of color change have been investigated. First, the effect of the substrate ($35Sub_{Au}$) concentration was studied, because it is the substrate strand that is physically responsible for the assembly of nanoparticles. It can be observed from Figure 3A that higher substrate concentrations resulted in faster color changes. To avoid decreased sensor sensitivity with too high substrate concentration, 3 nM of substrate was chosen for subsequent experiments, as a compromise between the detection time and sensitivity. Typically, 0.11 nM of 42-nm nanoparticles was used in each experiment, corresponding to a substrate-to-nanoparticle ratio of 27:1. Mirkin and co-workers have determined the number of DNA molecules attached to 16-nm gold nanoparticles to be 159 per particle.[53] Therefore, the number of DNA molecules on each of the 42-nm particles was estimated to be ~1100 per particle by assuming the same surface coverage.

The effect of the enzyme (17E) concentration was investigated next, while keeping other factors constant. As shown in Figure 3B, the rate of color change increased with an increase in enzyme concentration. In the absence of the enzyme, the aggregation was inhibited (Figure 3B, ■). This was somewhat unexpected since the substrate strand alone was thought to be physically responsible for the assembly of nanoparticles. The above enzyme-dependent studies suggest that the first step of the assembly process should be the hybridization of substrate strands to enzyme strands. After hybridization, a rigid backbone was formed on the substrate, forcing the two "sticky ends" of the substrate to stick out and facilitate the assembly of nanoparticles.[51] In the absence of the enzyme strand, the other "sticky end" might fold back to the same nanoparticle after a substrate hybridized with DNA on one nanoparticle, decreasing

(52) Reynolds, R. A., III; Mirkin, C. A.; Letsinger, R. L. *J. Am. Chem. Soc.* **2000**, *122*, 3795−3796.

(53) Demers, L. M.; Mirkin, C. A.; Mucic, R. C.; Reynolds, R. A., III; Letsinger, R. L.; Elghanian, R.; Viswanadham, G. *Anal. Chem.* **2000**, *72*, 5535−5541.

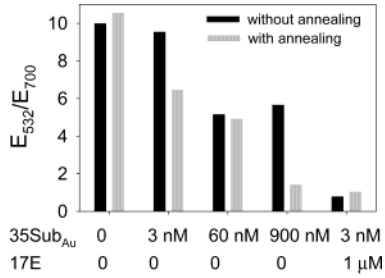

Figure 4. Comparison of the degree of aggregation with annealing (gray bars) or without annealing (black bars). The substrate (35Sub$_{Au}$) and enzyme (17E) concentrations for each experiment are indicated in the *x*-axis. Experimental conditions were similar to those described in Figure 2A. The samples were either annealed by warming to 55 °C for 5 min and subsequently cooling slowly to room temperature over 3 h or simply left at room temperature for 3 h.

the chance to anneal with another particle. To achieve a higher rate of color change at room temperature without annealing, high enzyme concentration (2 μM) was used to assist the substrate/enzyme hybridization, which corresponded to an enzyme-to-substrate ratio of 666:1.

One major advantage of the new design was elimination of the annealing step (a heating and cooling process). To gain further insight into the DNAzyme/nanoparticle system, the effect of annealing on the formation of nanoparticle aggregates was also investigated (see Figure 4). Several experimental conditions are shown on the horizontal axis. First, experiments were performed in the absence of the enzyme strand. With annealing for 3 h, the degree of aggregation increased with increasing substrate (35Sub$_{Au}$) concentration (gray bars). For samples sitting at room temperature for 3 h without annealing (black bars), the degree of aggregation was lower compared to samples with an annealing step, and the extinction ratio stopped decreasing when it reached ~5. These results suggested that for samples without the enzyme strand, an annealing step was important for the formation of large nanoparticle aggregates. However, in the presence of 1 μM of enzyme strand, the highest level of aggregation was observed even with only 3 nM of substrate, regardless of annealing or not. These observations were different from the results obtained for nanoparticles aligned in the "head-to-tail" manner, in which case no aggregation could be observed if the enzyme strand was missing, even with annealing.[51] The results confirmed that the alignment of nanoparticle is critical for accelerated nanoparticle aggregation at constant temperature. At the same time, the presence of an enzyme strand could help to increase the rate of aggregation significantly.

For a system containing gold nanoparticles functionalized with two different thiol-modified DNA, thiol-exchange reaction may occur, resulting in nanoparticles attached with both 3′- and 5′-thiol-modified DNA, which could bring the two "sticky ends" of the substrate to the same nanoparticle. In our system, the thiol exchange process was suppressed by two means. First, the two different nanoparticles were stored separately, so that the reaction time for thiol exchange was limited to about 10 min. Second, free thiol-modified DNA molecules were removed by multiple washing steps. The free thiol concentration was estimated to be less than 25 pM (see Experimental Section). It is known that the rate of thiol exchange is dependent on the concentration of free thiol. For example, the exchange rate was reported to be ~0.9 day^{-1} with ~1 mM of free thiol.[54] Since the estimated free thiol is much lower (<25 pM) and the detection time is very short (<10 min) in our system, the thiol exchange should be minimal.

The effect of NaCl concentration was also investigated. NaCl helps to reduce the electrostatic repulsion of negatively charged DNA phosphate backbones, and it thus favors DNA hybridization. As shown in Figure 3C, the rate of color change increased significantly with increasing NaCl concentrations. For example, the extinction ratio stopped decreasing in 3 min in the presence of 500 mM NaCl. Since large nanoparticles tend to aggregate by themselves irreversibly under high salt conditions and pose stability problems, a control experiment was performed to monitor the aggregation of the DNA-functionalized 42-nm nanoparticles in 500 mM NaCl by UV−vis spectroscopy. No significant decrease in the absorption was observed in 30 min, which was more than enough time to carry out the sensing operation (see Supporting Information, Figure S1). In practice, the DNA-functionalized nanoparticles were stored in a low salt condition (~100 mM NaCl) to maximize it stability (see Experimental Section) and were added to sensing solution containing high salt concentration right before sensing operation. For the current experiments, we chose to use 300 mM NaCl to reduce errors resulting from timing. In the presence of 300 mM NaCl, the extinction ratio decreasing was insignificant after ~10 min.

It is important to note that nanoparticle aggregates would continue to grow even though the extinction ratio stopped decreasing, because of reasons such as the growth of larger aggregates at the expense of smaller ones.[25] In theory, the change of aggregate size and size distribution can still cause a change in optical properties of the aggregates.[25] Therefore, it is difficult to define a state in which the aggregation is completely finished. In practice, when the extinction ratio drops to ~1, the rate for further decrease of the ratio is very slow (<0.1/min, see Figure 3). Therefore, the effect of further aggregate growth on detection should be minimal.

The Effect of Temperature. Ideal sensors should operate in a wide temperature range, including ambient temperature. Thus, the rate of nanoparticle aggregation at nine temperatures from 10 to 45 °C in the absence (Figure 5, □) and presence (■) of 2 μM Pb^{2+} were compared. The aggregation process was very slow at low temperature (10 °C, Figure 5A). It became faster with increasing temperature until 35 °C, after which a further increase of temperature resulted in decreased rates of aggregation to completely inhibited aggregation at 45 °C. Therefore, the rate of aggregation was strongly temperature-dependent. At each temperature, the solid squares were above the empty squares (except for 45 °C), indicating that the presence of Pb^{2+} inhibited nanoparticle aggregation. The optimal temperature for detection was determined to be 35 °C, where the two curves (■ and □) have the largest separation.

If the aggregation of nanoparticles at 25 °C (room temperature) and 35 °C are compared, detection at 35 °C has another advantage. At 25 °C, the sample with 2 μM of Pb^{2+} could also form aggregates, although with a slower rate (Figure 5D, □). After a sufficiently long time (i.e., 30 min), samples with or without Pb^{2+} would have almost identical color (Figure 5D).

(54) Hostetler, M. J.; Templeton, A. C.; Murray, R. W. *Langmuir* **1999**, *15*, 3782−3789.

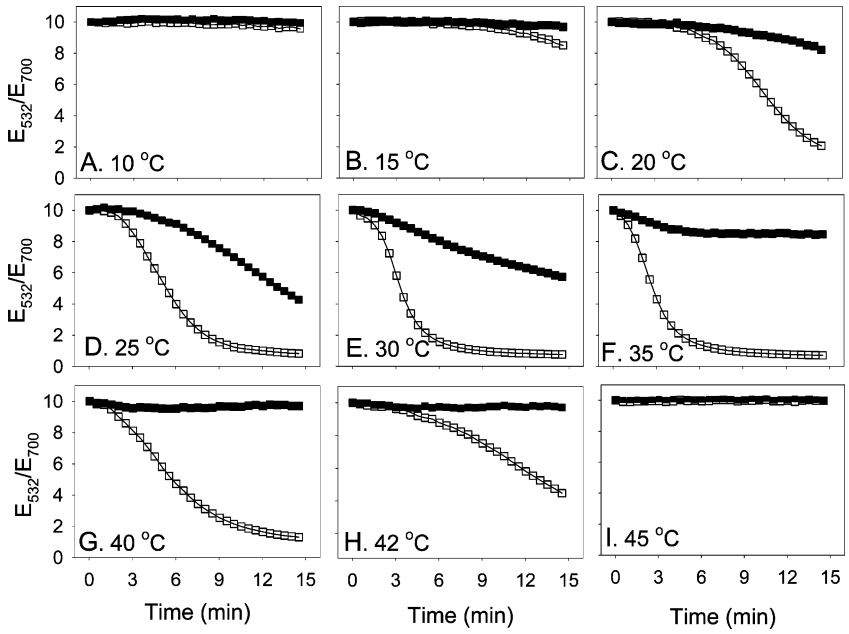

Figure 5. Temperature effect on the aggregation rate. (□) Obtained in the absence of Pb^{2+}; (■) obtained in the presence of 2 μM Pb^{2+}. Experimental conditions were similar to those described in Figure 2A, except that the temperature was varied.

On the other hand, at 35 °C the color of the sample with Pb^{2+} did not change after ~5 min (Figure 5F, ■). For practical applications, this stability in color is a valuable property. Although the sensor is based on the kinetics of DNAzyme cleavage and nanoparticle aggregation, it is capable of reaching an equilibrium state relatively fast. As a result, errors in timing would not induce significant errors in determining the detection results. The fact that ~35 °C is the optimal detection temperature allows the sensor to be used in a wide field temperature range, since 35 °C is a temperature readily obtainable by operator holding the sample tubes by hand even though the "room" or field temperature is different.

It was surprising that, at temperatures below 35 °C, the rate of aggregation decreased with decreasing temperature, since lower temperatures should stabilize the DNA duplex structure more. The observation can be explained as follows. For two pieces of DNA to hybridize, the secondary and tertiary structures of each individual piece have to be disrupted. As predicted by the Mfold program (available at the Bioinformatics Center at Rensselaer and Wadsworth web site, http://www.bioinfo.rpi.edu/applications/mfold),[55] no stable secondary structures were formed at 35 °C for the substrate strand ($35Sub_{Au}$). With decrease of temperature, more and more local structures were stabilized and the energy required to break these local structures (-dG) increased (see Supporting Information, Figure S2). Therefore, it is difficult for DNA to overcome the kinetic barrier of disrupting its own structure at lower temperature, resulting in a slower rate of nanoparticle aggregation. As a control experiment to demonstrate that the temperature-dependent aggregation was not confined to the DNAzyme system, a 24-mer DNA that was complementary to the two DNA strands on nanoparticles was used to assemble the nanoparticles at different temperatures. Results similar to the DNAzyme system were observed (see Supporting Information, Figure S3).

The Mfold program predicted non-cooperative transitions from 10 to 30 °C for the substrate (Figure S2). To check the temperature-dependent behavior of the substrate ($35Sub_{Au}$), its melting curve was measured, and the melting temperature was calculated to be 44 °C (Figure S2D). The higher experimentally measured transition temperature suggested that the Mfold program had missed certain stable secondary structures, which may be attributable to the fact that the single ribo-adenosine nucleotide (Figure 1A) was counted as a deoxy-ribo-adenosine for the Mfold calculation. The high melting temperature of the substrate could explain the need for the enzyme to assemble nanoparticles at 35 °C (Figure 3B). After annealing with the enzyme, the secondary structure of the substrate was disrupted. The substrate/enzyme complex could assemble nanoparticles more efficiently in comparison to the substrate alone, since the two "sticky ends" in the complex stretch out much more than in the substrate alone.

Performance of the New Pb^{2+} Sensor. Under the optimized detection condition (3 nM substrate, 2 μM enzyme, 300 mM NaCl, and 35 °C), the sensitivity and selectivity of the sensor were tested. The aggregation kinetics of the sensor with different Pb^{2+} concentrations was monitored by UV−vis spectroscopy. As shown in Figure 6A, the aggregation was close to completion after 8 min for the sample without any added Pb^{2+}. The aggregation was suppressed with increase of Pb^{2+} concentration. Therefore, extinction ratios at 8 min were used for quantification (Figure 6B). The extinction ratio has a linear relationship with Pb^{2+} in the concentration range from 0.4 to 2 μM. The selectivity of the sensor was checked by monitoring the rate of aggregation in the presence of 5 μM of different divalent metal ions (Figure 6C). Only Pb^{2+} could inhibit the aggregation of nanoparticles, while other metal ions showed aggregation rates similar to the background rate. Conveniently, the color of the sensor could be observed by spotting the resulting solution onto a solid substrate, such as an alumina TLC plate. Color progression from blue to red could be observed for samples with increasing Pb^{2+} concentration, while samples with 5 μM concentration of other metal ions gave blue-colored spots (Figure 6D).

(55) Zuker, M. *Nucleic Acids Res.* **2003**, *31*, 3406−3415.

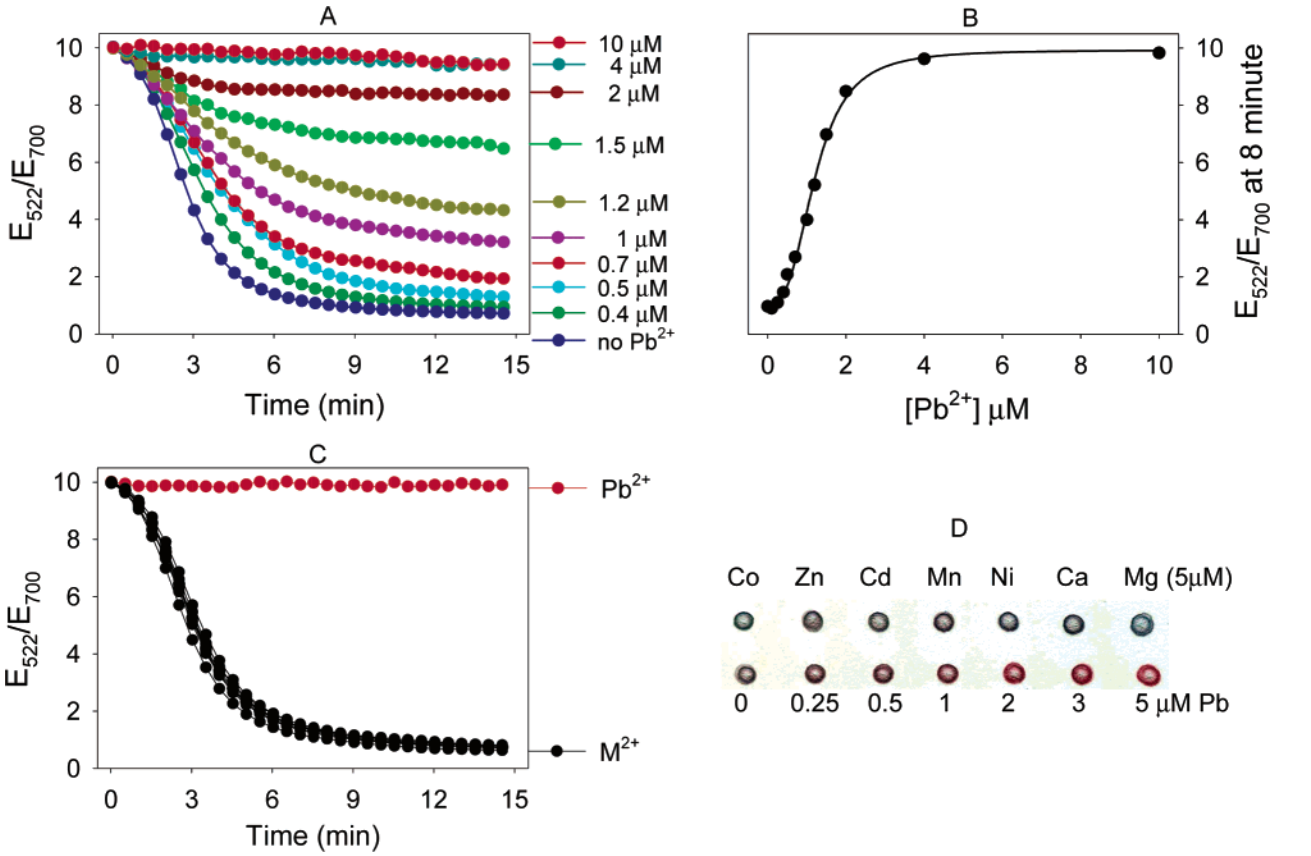

Figure 6. Sensitivity and selectivity of the new Pb^{2+} sensor. (A) Kinetics of nanoparticle aggregation in the presence of different Pb^{2+} concentrations. (B) Extinction ratio at 8 min after the initiation of aggregation for different Pb^{2+} concentrations (from Figure 6A). (C) Kinetics of nanoparticle aggregation in the presence of 5 μM of Pb^{2+} or other divalent metal ions (Co^{2+}, Zn^{2+}, Cd^{2+}, Mn^{2+}, Ni^{2+}, Ca^{2+}, and Mg^{2+}). (D) Color developed on an alumina TLC plate after 10 min of nanoparticle aggregation (see Experimental Section for details).

Conclusions

We have identified factors that affect the rate of color change of gold nanoparticles assembled by DNAzymes; this understanding has led to dramatically improved colorimetric sensors capable of fast (<10 min) detection at ambient temperature. Major factors that affect the rate of color change include the alignment and size of nanoparticles. The linking substrate, enzyme, and NaCl concentration as well as temperature also can affect the rate of color change. The sensor design method introduced here should be generally applicable to design colorimetric sensors with DNAzymes that show analyte-specific activities.

Experimental Section

Oligonucleotide and Reagents. All DNA samples were purchased from Integrated DNA Technologies Inc. The substrates and enzymes used in the experiments were purified by HPLC by the company. $Pb(OAc)_2 \cdot 3H_2O$ (99.999%), $HAuCl_4$ (99.999%) and sodium citrate dihydrate (99+ %) were purchased from Aldrich and used without further purification.

Preparation and Functionalization of Gold Nanoparticles. Gold nanoparticles (42-nm diameter) were prepared by the reduction of $HAuCl_4$ by sodium citrate.[56] Glassware used in the preparation was soaked in aqua regia and rinsed thoroughly with Millipore water. In a 250-mL two-neck flask, 200 mL of 0.3 mM $HAuCl_4$ was heated to reflux with stirring; 1.8 mL of 38.8 mM sodium citrate was then added. Within several minutes, the color changed from pale yellow to deep red. After the color change, the system was allowed to reflux for another half hour to allow complete reduction. Then the system was cooled slowly to room temperature, and the nanoparticles were filtered with a funnel (Pyrex). The nanoparticles were characterized with TEM (JEOL 2010), and the size was determined to be 42 ± 6 nm. Most of the nanoparticles had a spherical shape, and a small portion of nanoparticles appeared to be nanorods with aspect ratio less than 2. The gold colloid had an extinction peak at 532 nm of ~1.04, and the concentration was calculated to be approximately 0.13 nM, using the assumption that all nanoparticles were spherical with radii of 42 nm, all $HAuCl_4$ was reacted, and the density of nanoparticles was the same as bulk gold. This gave an extinction coefficient of 8.0×10^9 M^{-1} cm^{-1} at 532 nm. For 35-nm diameter gold nanoparticles, similar procedures for the preparation were used, except that 2.0 mL of sodium citrate, instead of 1.8 mL, was added.[56] The preparation of 13-nm diameter nanoparticles followed literature procedures.[57]

Functionalization of Nanoparticles with 3′- or 5′-Thiol-Modified DNA. Thiol-modified DNA was activated by incubating with 100 mM DTT. Typically, 60 μL of 1 mM DNA was incubated with 60 μL of 200 mM DTT at room temperature for 1 h. The mixture was then diluted with water to 600 μL and was desalted with a Sep-Pak C18 column (Waters) to remove DTT. The column was treated sequentially with 10 mL of 95% CH_3CN, 10 mL of mixture of CH_3CN, methanol, and water (1:1:1 volume ratio), 20 mL of water, and 10 mL of 2 M NH_4-OAc. The DNA and DTT mixture was then loaded into the column. DTT was washed away by 20 mL of water, and DNA was eluted by 1 mL of elution solution (containing 1:1:1 volume ratio of CH_3CN,

(56) Handley, D. A. In *Colloidal Gold Principles, Methods, and Aplications*; Hayat, M. A., Ed.; Academic Press: San Diego, CA, 1989; Vol. 1, pp 1−12.

(57) Storhoff, J. J.; Elghanian, R.; Mucic, R. C.; Mirkin, C. A.; Letsinger, R. L. *J. Am. Chem. Soc.* **1998**, *120*, 1959−1964.

methanol, and water). The eluted DNA was added to 12 mL of gold nanoparticles (~0.13 nM). The concentration of thiol-modified DNA was ~3 μM after the DTT treatment and desalting. After incubation for 1 day, 1.4 mL of buffer containing 1 M NaCl and 0.1 M Tris acetate, pH 8.2, was added by drop. After another incubation of 2 days, the nanoparticles were purified by centrifugation at 8000 rpm for 15 min. The supernatant (~98% of total volume) was removed, and DNA-functionalized nanoparticles were redispersed in 25 mM Tris acetate buffer, pH 8.2, with 100 mM NaCl. The process was repeated three times to minimize free DNA in solution. The concentration of free DNA was estimated to be less than 25 pM with the three washing steps. Finally, the nanoparticles were dispersed in the same buffer, and the extinction at 532 nm was adjusted to ~2.2 (corresponding to a concentration of ~0.28 nM for 42-nm nanoparticles and ~0.5 nM for 35-nm nanoparticles).

Assembly of Nanoparticles by the DNAzyme. In a typical experiment, 20 μL of nanoparticles functionalized with 3′-thiol-modified DNA (3′DNA_{Au}) and 20 μL of nanoparticles functionalized with 5′-thiol-modified DNA-functionalized gold nanoparticles (5′DNA_{Au}) were mixed (both with extinction at 532 nm of ~2.2). NaCl, the enzyme (17E), and divalent metal ions to be detected were added, and the final volume was adjusted to 98 μL. The aggregation was initiated by adding 2 μL of substrate strand, and the extinction was monitored on a Hewlett-Packard 8453 spectrophotometer. The buffer was Tris acetate (pH 8.2). The dead time between adding the substrate to the monitoring of the first spectrum was controlled to be 15 s for all samples.

Spot Test on TLC Plates. Typically, for 10 μL of 0.22 nM of 3′DNA_{Au} and 5′DNA_{Au} mixture containing 300 mM NaCl and 2 μM 17E with varying divalent metal ion concentrations, 1 μL of 50 nM substrate ($35Sub_{Au}$) was added to initiate aggregation. After 10 min, the solution was spotted onto an alumina TLC plate. After drying, the plate was scanned with a scanner (Canon 5000F).

Acknowledgment. This material is based upon work supported by the U.S. Department of Energy (NABIR program, DEFG02-01-ER63179), National Science Foundation (DMR-0117792 and CTS-0120978), and Department of Housing and Urban Development (ILLTS0097-03).

Supporting Information Available: Nanoparticle stability assay in 500 mM NaCl, predicted secondary structures of the $35Sub_{Au}$ at different temperatures, temperature-dependent aggregation of gold nanoparticles by a complementary DNA, and a melting curve of the DNAzyme-assembled nanoparticle aggregates. This material is available free of charge via the Internet at http://pubs.acs.org.

JA046628H